Mapping Frost-Sensitive Areas with a Three-Dimensional Local-Scale Numerical Model. Part II: Comparison with Observations

R. AVISSAR

Department of Atmospheric Science, Colorado State University, Fort Collins, Colorado

Y. MAHRER

Seagram Centre for Soil and Water Sciences, Faculty of Agriculture, Hebrew University of Jerusalem, Rehovot 76100, Israel

(Manuscript received 28 March 1987, in final form 23 October 1987)

ABSTRACT

A three-dimensional numerical model was developed to predict the microclimate near the ground surface of local-scale domains during radiative frost events. Its performances are compared with an observational topoclimatological survey of minimum temperatures at a height of 0.5 m above the soil surface which was carried out, during radiative frost events, in the Hefer Valley, Israel. Considering only topography and soil type in the numerical simulation, relatively good agreement is obtained between predicted and observed minimum temperatures. A more realistic picture is given when vegetation is incorporated in the model, although larger discrepancies with observations are obtained. This is mainly explained by the fact that measurements were always carried out above bare surfaces, even when dense vegetation was present and, therefore, do not provide a representative minimum temperature of many areas. This assumption is validated by field measurements of nighttime temperatures in an orchard and above a bare soil in its immediate vicinity.

1. Introduction

Radiative frost is one of the most severe weather conditions that affects agricultural activities in many parts of the world. Since various protective methods to reduce frost impact are available (Blanc et al., 1963; Turrell, 1973; Bagdonass et al., 1978), refinements of frost-forecasting methodologies should provide economical benefits. In the first part of this study (Avissar and Mahrer, 1988; hereafter referred to as Part I), a three-dimensional local (meso-γ) scale numerical model was suggested as an alternative method to topoclimatological surveys of air minimum temperature at 0.5 m height above the soil surface. These surveys require an extended network of observations over a period of several years and, consequently, are very tedious and expensive (Schnelle, 1950; Geiger, 1966; Hogg, 1966, 1968; Lomas and Gat, 1971; Suzuki et al., 1982). The model is based on the equations of motion, heat, humidity and mass continuity in the atmosphere, and the equations of heat and moisture diffusion in the soil. It predicts the microclimate near the ground of complex terrain during radiative frost events and particularly the foliage temperature which should be considered for mapping frost-sensitive areas instead of the commonly used air temperature (Part I). Using this model, it was demonstrated that the predicted air temperature at a height of 0.5 m above the soil surface is influenced by plant cover, soil type and moisture content, air specific humidity, wind speed and topography. Similar conclusions, based on observations (Blanc et al., 1963; Lomas and Gat, 1971; Bootsma, 1976; Bagdonass et al., 1978; Von Lengerke, 1978; Suzuki et al., 1982; Kalma et al., 1983; Goldsworthy and Schulman, 1984), emphasize the model's ability to correctly predict the general trends of the microclimate near the soil surface under radiative frost conditions. The aim of the second part of this study is to compare the model performances with a topoclimatological survey that was carried out, during the 1960s, in Hefer Valley (Israel) by the Meteorological Service of Israel. This survey was described in detail by Lomas and Gat (1971) and is summarized in section 2.

2. Observational survey analysis

Topoclimatological surveys of minimum temperature at a height of 0.5 m above soil surface during radiative frost events are carried out in four stages (Lomas and Gat, 1971):

(i) Planning. The site of local measuring stations is determined according primarily to topography and soil type. One station, representative of the climatological region, is also designated (referred to as the "main station").

Corresponding author address: Dr. Roni Avissar, Dept. of Atmospheric Science, Colorado State University, Fort Collins, CO 80523.

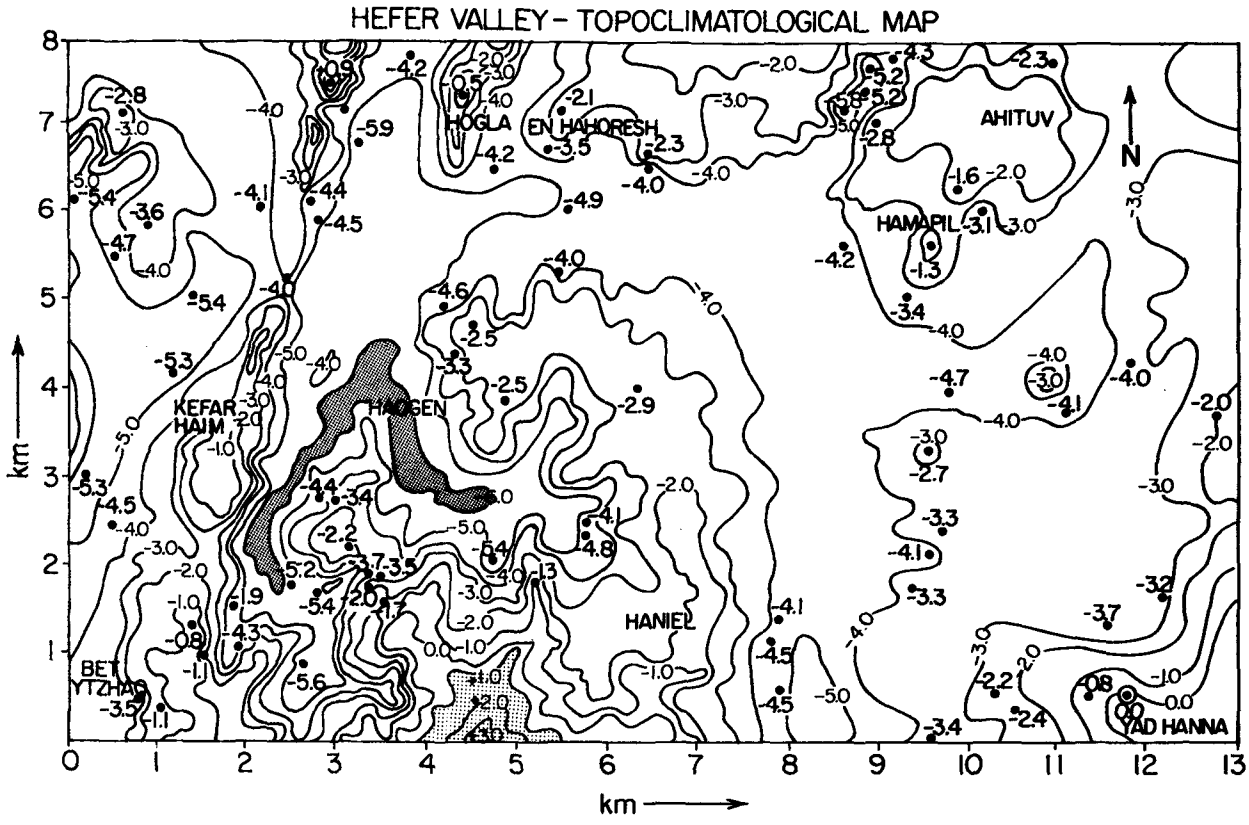

FIG. 1. Topoclimatological map of Hefer Valley (Meteorological Service of Israel, 1965–69).

(ii) Field measurements. In order to obtain statistically sound results, measurements must be collected for at least 4 or 5 yr during the relevant season.

(iii) Data analysis and mapping. Observed minimum temperatures of all relevant seasons are selected according to the following criteria:

- minimum temperature in the main station below 5°C,
- cloudiness less than 3/8 during the early morning,
- wind speeds not stronger than 1.5 m s^{-1} during the early morning, and
- a relatively large temperature gradient near the soil surface.

(iv) Averaging. All the minimum temperatures recorded according to (iii) for each station are averaged in order to get the mean minimum temperature of the station.

A statistical analysis is then accomplished on the mean minimum temperature differences between the main and each of the local stations. These differences are used to design the topoclimatological maps.

Figure 1 presents the topoclimatological map of Hefer Valley derived from the map prepared by the Meteorological Service of Israel, according to measurements of minimum temperatures carried out at 71 local stations during radiative frost events between 1965 and 1969. The highest temperature on this map is about 3°C and the coldest is about −6°C. Black points indicate site of the local stations and the adjacent number is the mean difference temperature from the main station (Yad Hanna) which is designated by a double circle. Isotherms were drawn according to the topography of the domain.

Figures 2, 3 and 4 illustrate the topography, soil types and soil covers of Hefer Valley, respectively, with a resolution of 500 m × 500 m. Figure 2a is a general view of the region and Fig. 2b is the detailed topography of the domain considered in this observational survey. Its origin (0, 0) is located at 32°19′N, 34°53′E. The lowest elevation is 13 m MSL and the highest is 62 m MSL. Figure 3 was obtained from the map of soil types of Israel (Ravikovitch, 1969) by averaging soil types over areas of 500 m by 500 m. Figure 4 was obtained, in a similar way, from recent 1:10 000 maps of the region.[1] Representativeness of the measuring stations in the domain was tested by relating their distribution with topography (Fig. 5), soil types (Fig. 6) and soil cover types (Fig. 7). From this verification, it is obvious that, in general, the distribution of the stations is statistically sound. It should be noted, however, that there are no stations in the highest elevations of the domain, or in the vicinity of the large fish ponds. The relationship between minimum temperature differences and

[1] Maps published by Survey Department of Israel.

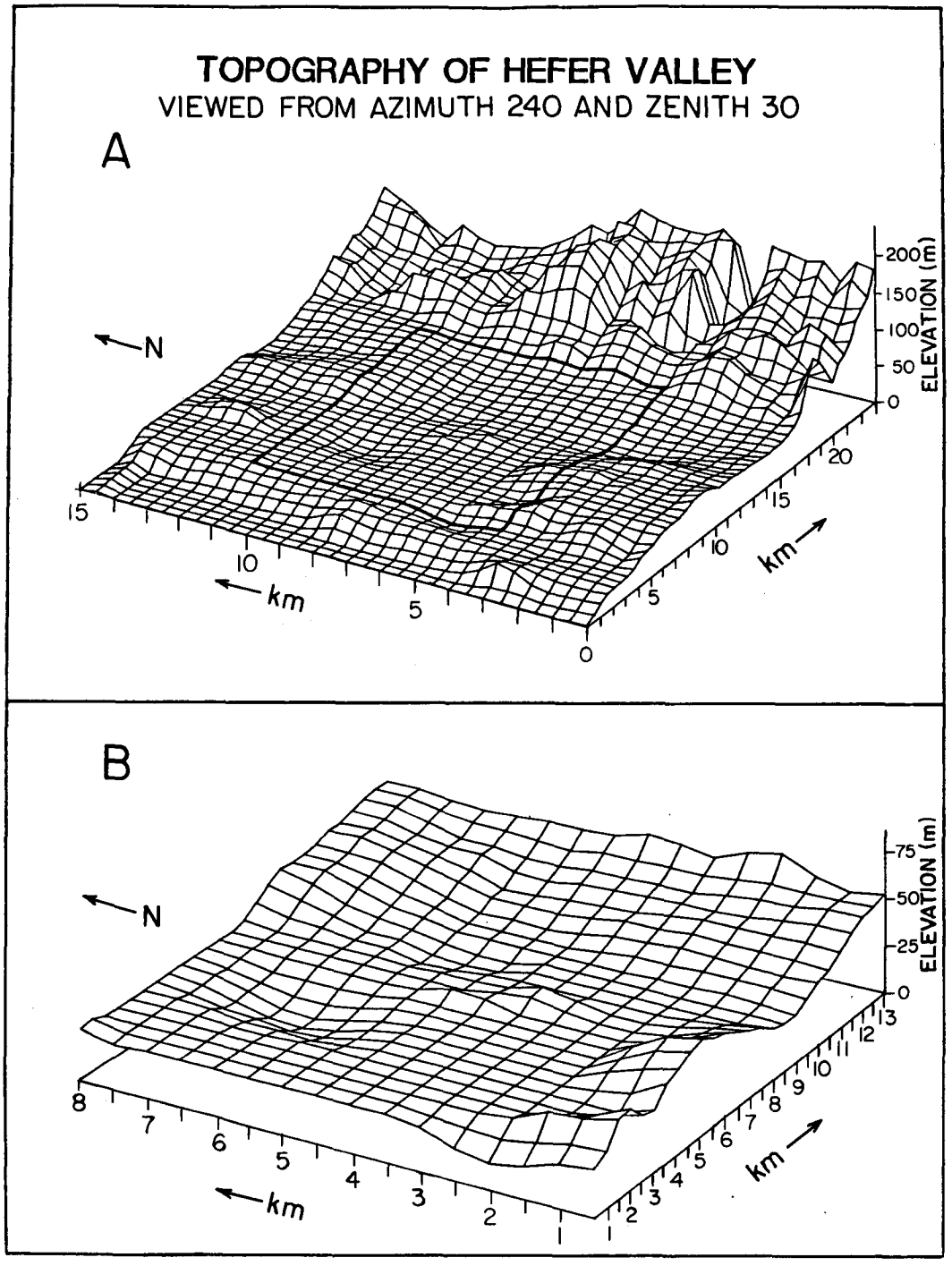

FIG. 2. Topography of Hefer Valley with a resolution of 500 m. (a) General view of the region, and (b) domain of the survey.

elevation of the stations is presented in Fig. 8. The low correlation found between these two parameters (r^2 = 0.13) emphasizes that they are not significantly related, although their linear regression shows a trend of temperature increasing with elevation. Figures 9 and 10 show that neither soil type nor soil cover type may explain the variation of temperature between the local stations of the domain. The combined effects of topography, soil type and soil cover versus minimum temperature in the stations were tested with a multiple regression model. In only 37% of the stations, a significant correlation was found between these parameters. As was already emphasized in the first part of this study, other parameters such as wind speed, air

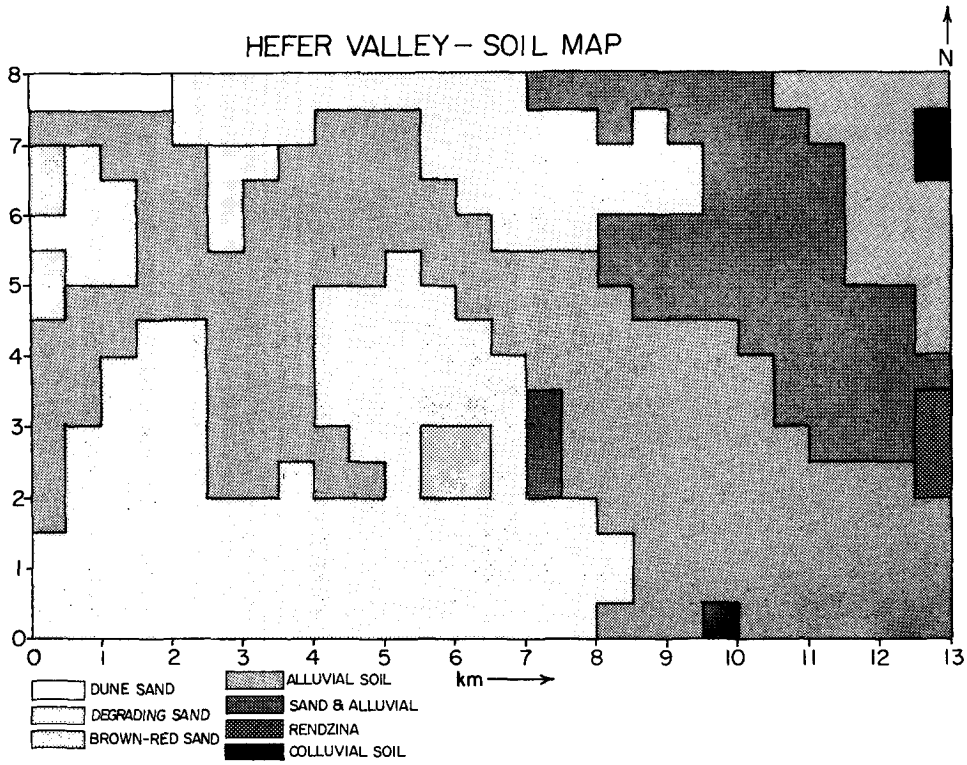

FIG. 3. Soil map of Hefer Valley with a resolution of 500 m (Ravikovitch, 1969).

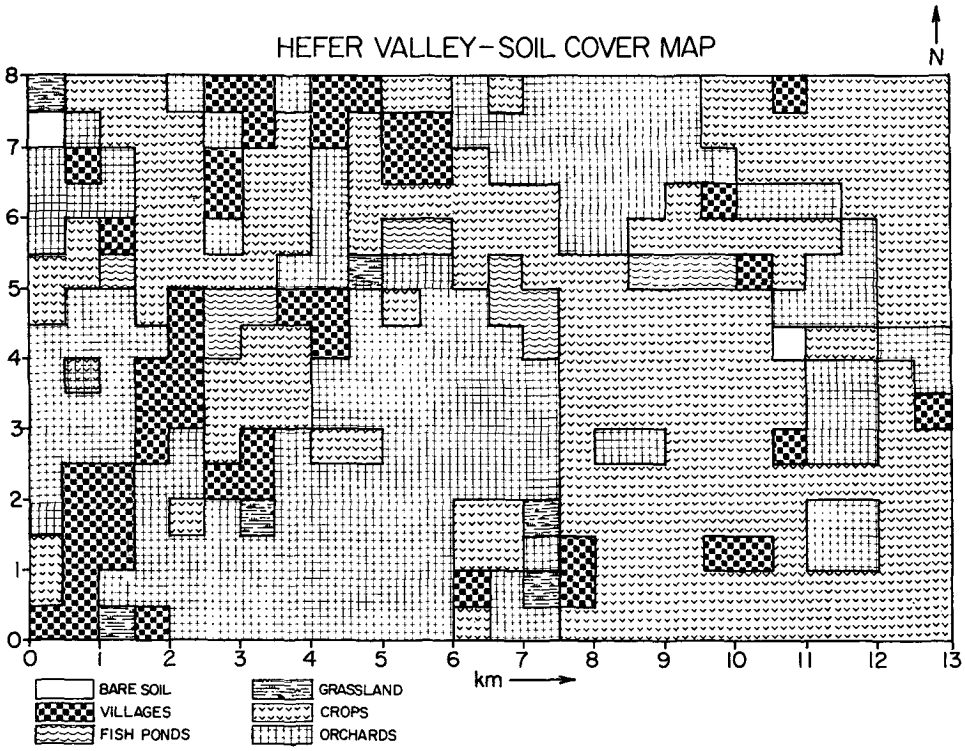

FIG. 4. Soil cover map of Hefer Valley with a resolution of 500 m.

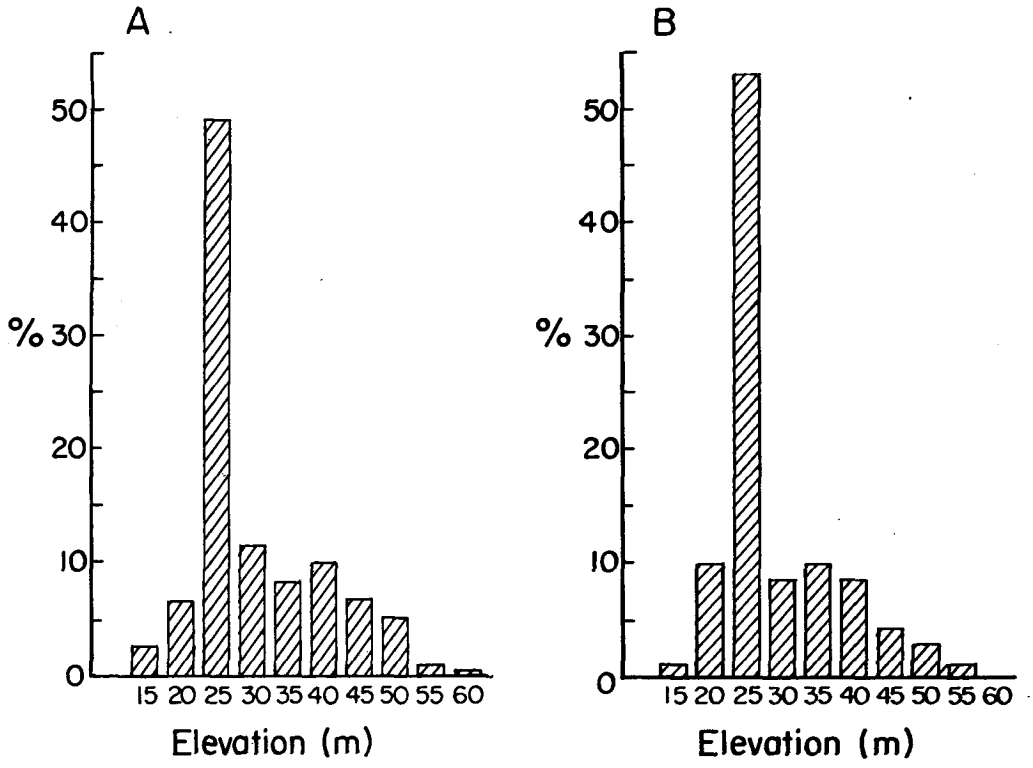

FIG. 5. Distribution of (a) heights of Hefer Valley and (b) the measuring stations by heights.

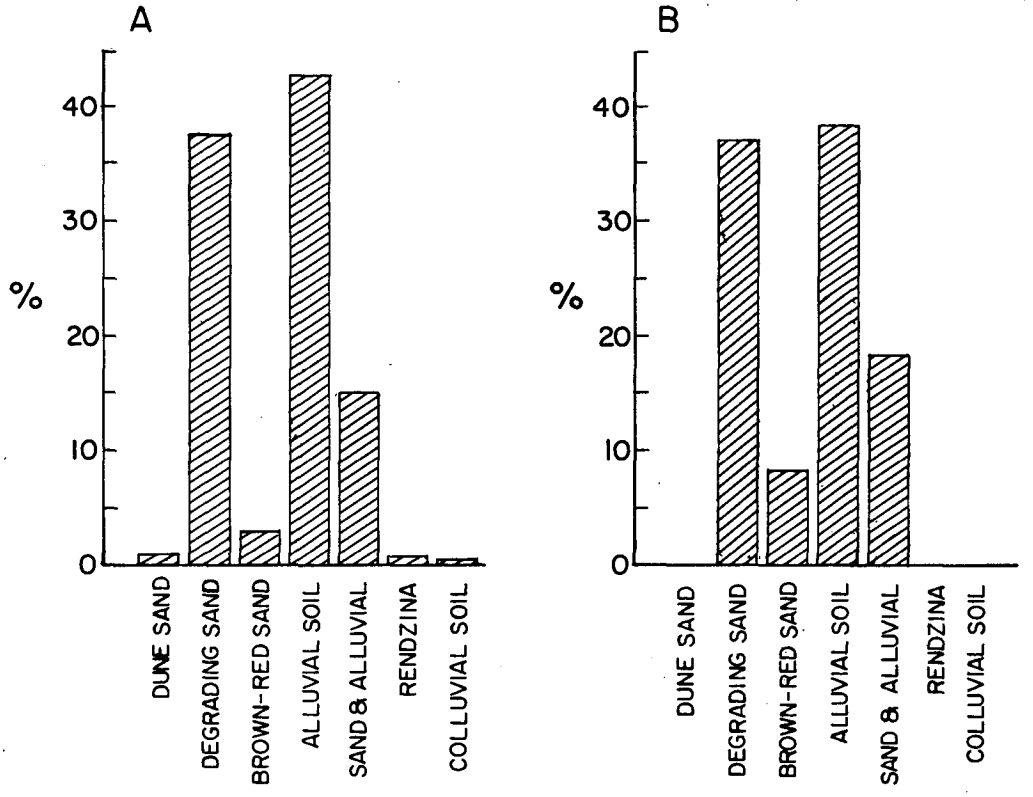

FIG. 6. As in Fig. 5, except for soil types.

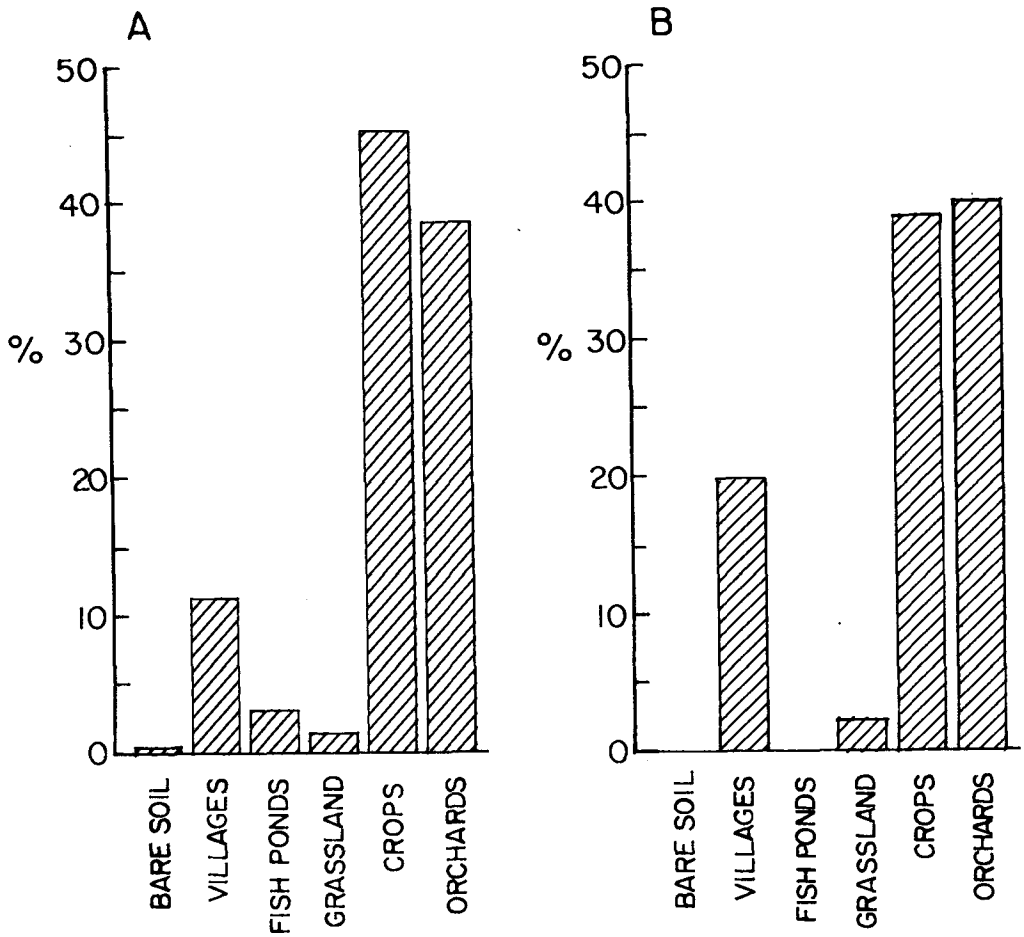

FIG. 7. As in Fig. 5, except for soil-cover types.

humidity or soil wetness should be considered together with the above parameters to explain the variance between all the stations.

3. Numerical experiment

In order to compare the model results with the observational survey of Hefer Valley, the model was integrated in its three-dimensional version. The radiosonde data used to initialize the model were averaged from 20 radiosondes released at Bet-Dagan (Israel) at 2400 LST during radiative frost events in which measurements were carried out for the establishment of the topoclimatological survey. These radiosondes were selected because of their similarity and their representativeness of typical radiative frosts in Israel. The deviation between each radiosonde and the average value

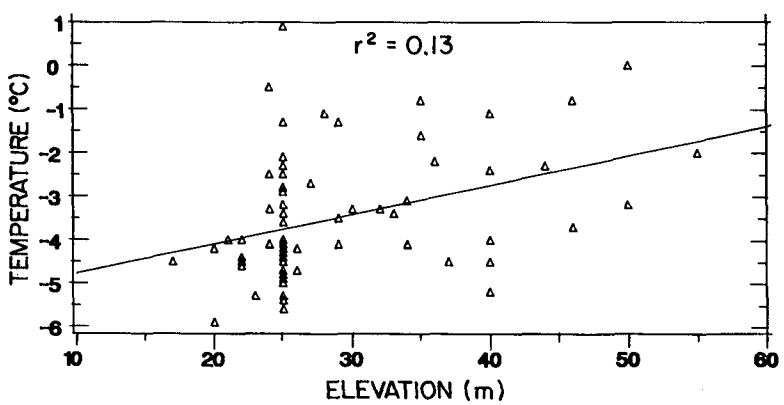

FIG. 8. Relation between minimum temperature and topography in Hefer Valley.

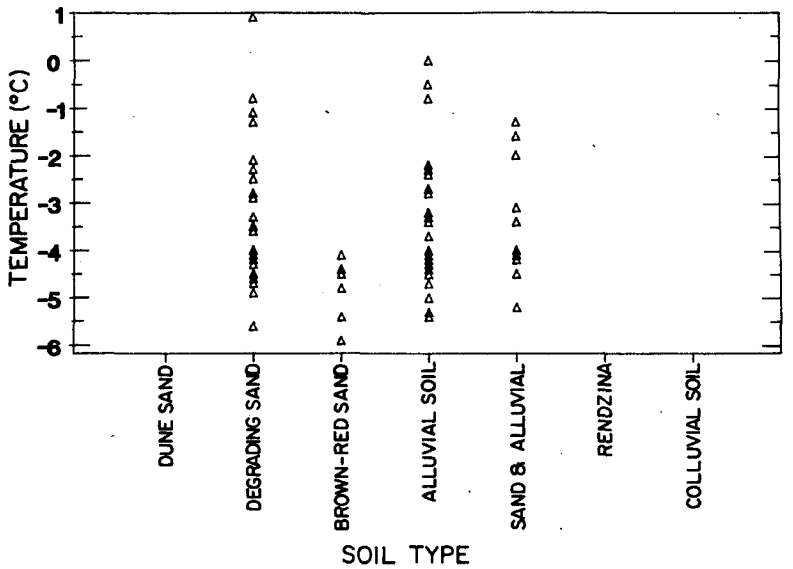

FIG. 9. As in Fig. 8, except for minimum temperature and soil type.

was small and, therefore, probably does not affect the microclimate near the ground surface. These data are presented in Fig. 11. At each grid point of the model we defined the topography, soil type and soil cover of Hefer Valley according to the maps presented in Figs. 2, 3 and 4, respectively. Although predicted and observed data are compared in the domain represented in Fig. 2b, the model was run for the domain represented in Fig. 2a in order to account for the circulation generated by the topographical features. Properties of the various soil and cover encountered in these maps are listed in Tables 1 and 2, respectively. Soil temperature at the lowest boundary of the model (1 m depth) was assumed constant during the simulation and equal to 15°C according to Zemel and Lomas (1977). Soil water potential, at this boundary, was also assumed to be constant and equal to −3.3 m which is the value at "field capacity". Initial temperature and moisture profiles, in each soil, were obtained by running the model in its one-dimensional version, starting with uniform vertical profiles, for 48 h preceding the frost events. The horizontal distance between two grid points was 500 m. In the vertical, 19 levels at 0, 0.5, 2, 5, 10, 25, 50, 100, 200, 400, 600, 800, 1000, 1250, 1500, 1750, 2000, 2500 and 3000 m were considered in the atmosphere and 20 levels with increments of 0.05 m each, between soil surface and a depth of 1 m, were considered in the soil. The time step for the integration of the model equations was 20 s. In order to get the minimum temperature at each location of the domain, the model was run for 6 h, starting at 2400 LST.

Figure 12 presents predicted versus observed differences of minimum temperatures between the main and the 71 local stations at a height of 0.5 m above the soil

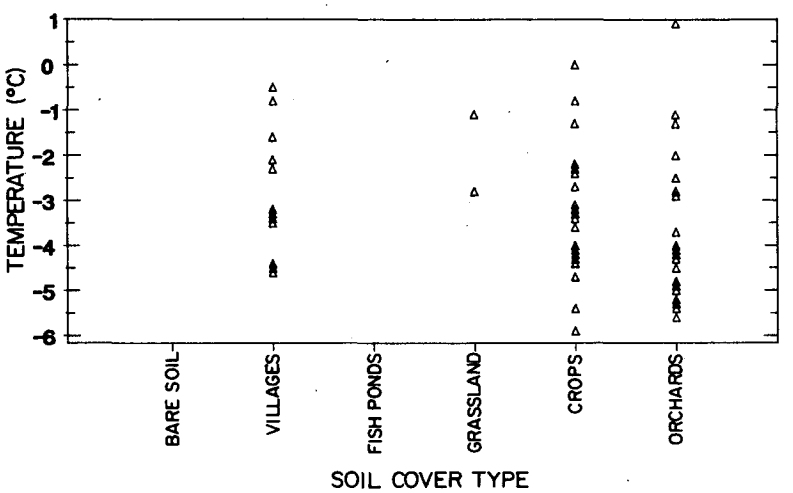

FIG. 10. As in Fig. 8, except for minimum temperature and soil cover.

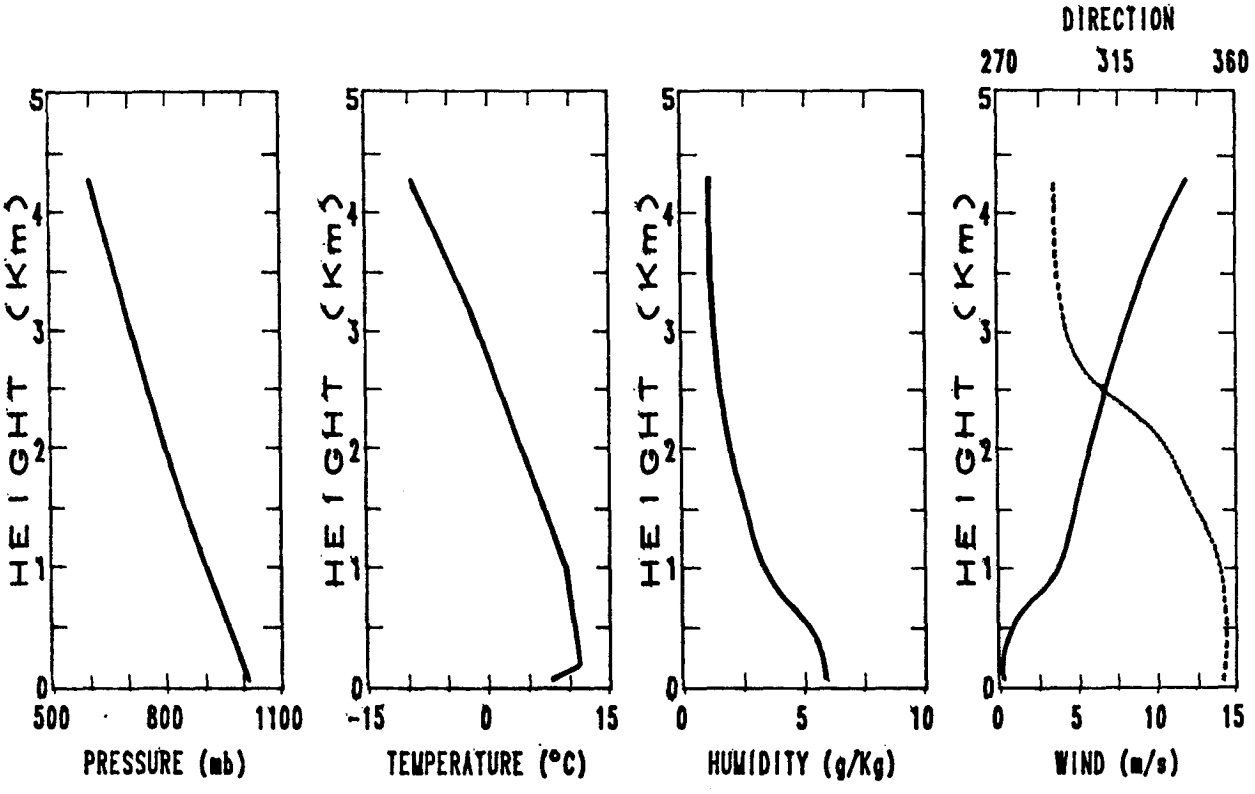

FIG. 11. Averaged meteorological conditions obtained from 20 radiosondes released at Bet-Dagan, Israel, during radiative frost conditions.

surface. A relatively low correlation was found between them ($r = 0.65$) although, on the basis of a one-tailed test of the Student's t distribution, it may be noted that at a significance level of 0.005, this correlation coefficient is significantly greater than zero since $t > t_{.995}$ for $71 - 2 = 69$ degrees of freedom. The discrepancies

TABLE 1. Properties of the different soils of Hefer Valley. Here K_{hs} is the hydraulic conductivity at saturation; ψ_{cr} the critical matrix potential; θ_r and θ_s are the residual and saturation water contents, respectively; and n and m are empirical constants specific to each soil (Part I).

		Soil types						
Property	Units	Dune sand	Degrading sand	Brown-red sand	Alluvial soil	Sand and alluvial	Rendzina	Colluvial soil
Texture								
Sand	%	98	93	87	60	70	40	30
Silt	%	1	3	5	15	11	25	25
Clay	%	1	3	6	20	16	30	40
Organic matter	%	0	1	2	5	3	5	5
Density	kg m^{-3}	1200	1250	1300	1500	1600	1600	1650
Hydraulic properties								
K_{hs}	m day^{-1}	2.0	1.5	1.0	0.1	0.5	0.08	0.05
n	—	2.5	3.0	3.5	6.0	4.5	8.0	10.0
m	—	2.0	1.5	0.83	0.5	0.7	0.4	0.3
ψ_{cr}	m	−0.05	−0.1	−0.15	−0.5	−0.3	−0.7	−1.0
θ_s	m^3 m^{-3}	0.3	0.4	0.4	0.4	0.4	0.45	0.50
θ_r	m^3 m^{-3}	0.01	0.01	0.02	0.05	0.03	0.05	0.05
Photometric properties								
shortwave radiation								
albedo	—	0.25	0.22	0.2	0.18	0.19	0.25	0.18
absorbance	—	0.75	0.78	0.8	0.82	0.81	0.75	0.82
longwave radiation								
reflectance	—	0.1	0.1	0.1	0.1	0.1	0.1	0.1
absorbance	—	0.9	0.9	0.9	0.9	0.9	00.9	0.9
emissivity	—	0.9	0.9	0.9	0.9	0.9	0.9	0.9

TABLE 2. Properties of the different soil covers of Hefer Valley.

Property	Units	Cover type			
		Village	Grassland	Crops	Orchards
Shielding factor (σ_f)	—	0.50	0.25	0.75	0.90
Leaf area index	—	2.0	2.0	3.0	8.0
Vegetation height	m	0.20	0.40	1.0	3.0
Photometric properties (single leaf)					
shortwave radiation					
albedo	—	0.25	0.25	0.20	0.20
absorbance	—	0.35	0.35	0.40	0.40
transmittance	—	0.40	0.40	0.40	0.40
Longwave radiation					
reflectance	—	0.08	0.08	0.08	0.08
absorbance	—	0.92	0.92	0.92	0.92
emissivity	—	0.92	0.92	0.92	0.92

obtained between predicted and observed values are mainly due to the fact that observations were always carried out in open areas, even when most of the area around the station was covered with dense vegetation. Since during radiative frost events the atmosphere is very stable and advective effects are generally negligible due to weak winds, the temperature measured at the station is only representative of the immediate vicinity of the thermometer and, unlike the numerical model, does not give an average value of the considered grid. Therefore, the divergence between predicted and observed minimum temperatures increases with the density of the vegetation. In order to demonstrate this phenomenon, a field experiment was carried out in the orchard of the experimental farm of the Faculty of Agriculture at Rehovot, Israel, during spring 1986. The trees at this location are 3 m high, have a leaf area index of 6, and cover about half of the area ($\sigma_f = 0.5$). Air temperature was measured, in three replicates, with thermocouples at 0.5 m height above the soil surface. One set of measurements was carried out in the ambient air of the canopy, and another above the bare soil between two rows of trees in the middle of the orchard. A third set of measurements, which also included wind speed at 2 m height, was taken in a bare field adjacent to the orchard at a distance of 50 m from the edge of the orchard. The temperatures and wind speed were integrated and then averaged over periods of 30 min. The difference between the mean temperature in and outside the orchard during a representative night of the season is presented in Fig. 13. Although there were no frost conditions during this period, significant differences can be observed between these areas. Under radiative frost conditions, more pronounced differences are expected due to the lack of turbulence and a larger radiative cooling of the emitting surfaces. It is interesting to note that when the wind is weak, the temperature in the orchard is lower than in the bare field, while even with a light wind, it is the opposite. This surprising phenomenon, also predictable by the model, is explained by the fact that the coldest point in the vertical profile of temperature over bare soil is the surface (with a shallow stable layer near the ground), while rapid radiative cooling of trees results in a minimum at some height inside the canopy and a warmer surface (Fig. 14a). Effects like advection and increasing turbulence, due to wind speed, generate more homogeneous profiles of temperature, especially in the presence of trees which increase the surface roughness and result in a warmest temperature at 0.5 m height above the soil surface (Fig. 14b). These results are supported by the observational (Hauf and Witte, 1985) and numerical (Gross, 1987) studies of production of cold air during the night, above bare soils and surfaces covered by trees. Larger productions of cold air are obtained above covered surfaces due to the larger

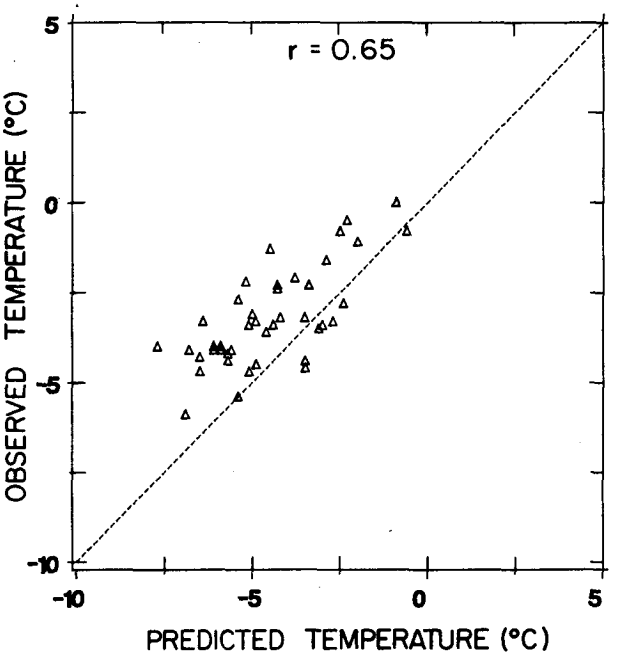

FIG. 12. Predicted and observed differences of minimum temperatures in Hefer Valley.

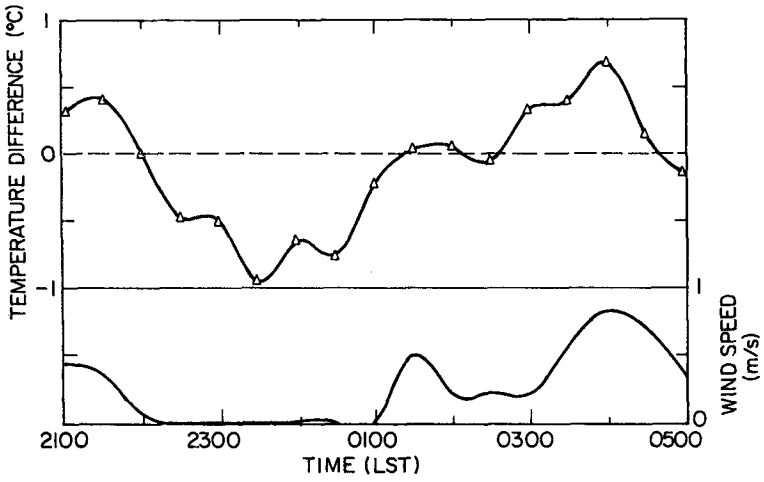

FIG. 13. The variation of the difference of air temperature between an orchard and an adjacent bare field during a spring night in central Israel.

"active surface" of the trees and, consequently, larger sensible heat fluxes from the atmosphere.

These results also emphasize the difference between canopy and air temperatures.

The three-dimensional model was integrated assuming that all the soils of Hefer Valley were bare (i.e., without considering the influence of vegetation, water ponds and villages), thus, approaching the observational survey conditions. As can be seen in Fig. 15, a better correlation ($r = 0.76$) was obtained between predicted and observed differences of minimum temperatures between the main and the local stations, reinforcing our assumption.

Another reason for the discrepancies obtained between predicted and observed minimum air temperatures may be attributed to the fact that, in a few places of the studied domain, the use of frost-protective methods may have increased the measured temperatures and, through lack of information, was not considered in the simulations. It should be noted, finally, that rows of tall trees (or other windbreaks) may have a strong influence on the wind flow and, consequently,

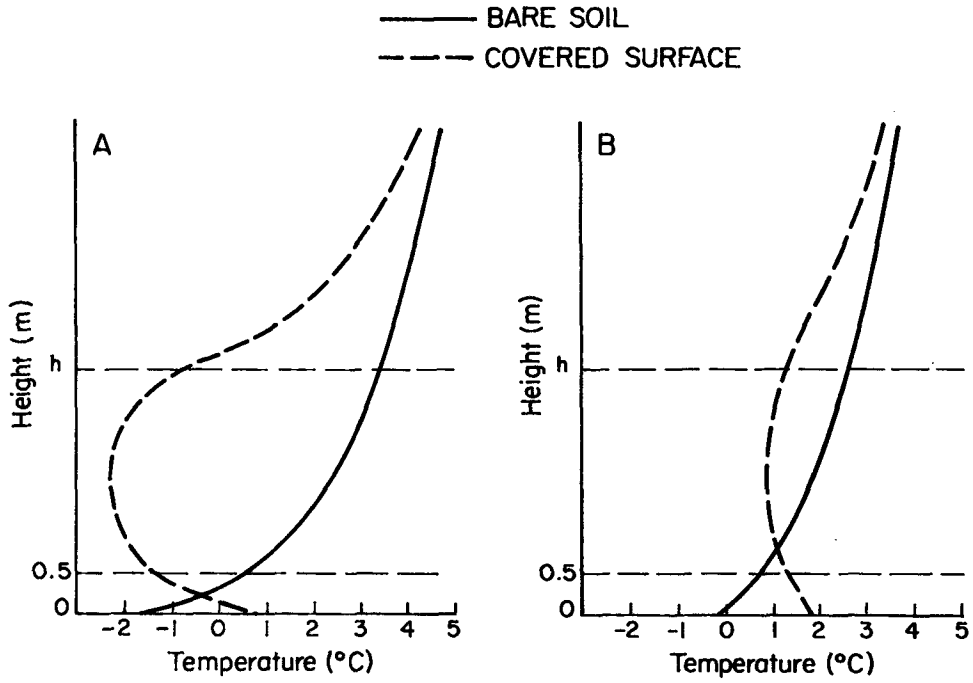

FIG. 14. Typical profile of temperature near the ground surface during nighttime with (a) weak wind, and (b) strong wind. Here h indicates the top of the canopy.

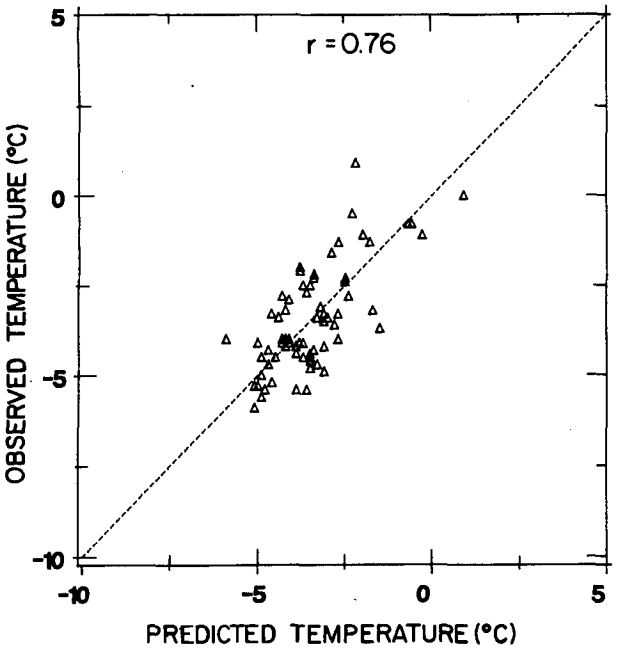

FIG. 15. As in Fig. 12 except for the bare Hefer Valley.

the microclimate of specific areas. Due to the "bulk" parameterization of the vegetation in the model, they are not correctly represented. This may be corrected, however, by incorporating in the model a more sophisticated parameterization of the soil–plant–air system which will account for two- or three-dimensional inhomogeneities.

Figures 16 and 17 present the simulated topoclimatological maps of Hefer Valley when considering (Fig. 16), and not considering (Fig. 17), the soil covers. The comparison between these two figures emphasizes the significant influence of dense vegetation and water ponds on the minimum temperature near the ground surface. The greatest discrepancies between these two maps are obtained at the water ponds where the temperature during the night is much higher than for bare and vegetated soils. It may be seen, again, that the map obtained for the "bare" case is more similar to the observed map presented in Fig. 18 which, in order to be compatible with the model resolution, was obtained from Fig. 1 by averaging temperatures over areas of 500 m × 500 m. Since there were no measuring stations in the highest elevations of the domain and the temperatures of the observational survey were extrapolated only according to topography, discrepancies obtained at these locations are not surprising.

4. Summary and conclusions

The three-dimensional numerical model for mapping frost-sensitive areas described in Part I was compared here with an observational survey. A statistical analysis of the survey showed that there is no simple linear correlation between minimum temperature and topography (and not even with the combined effect of topography, soil type and soil cover). Therefore, any attempt to map frost-sensitive areas by using such considerations seems to be insufficient. In order to be applicable with reasonable accuracy, an observational survey of inhomogeneous areas like Hefer Valley should include a much more refined grid of measurements. However, for objective reasons, it does not seem possible.

From a practical point of view, it is more important to know the temperature of the vegetation than the air temperature at 0.5 m height which may even be mis-

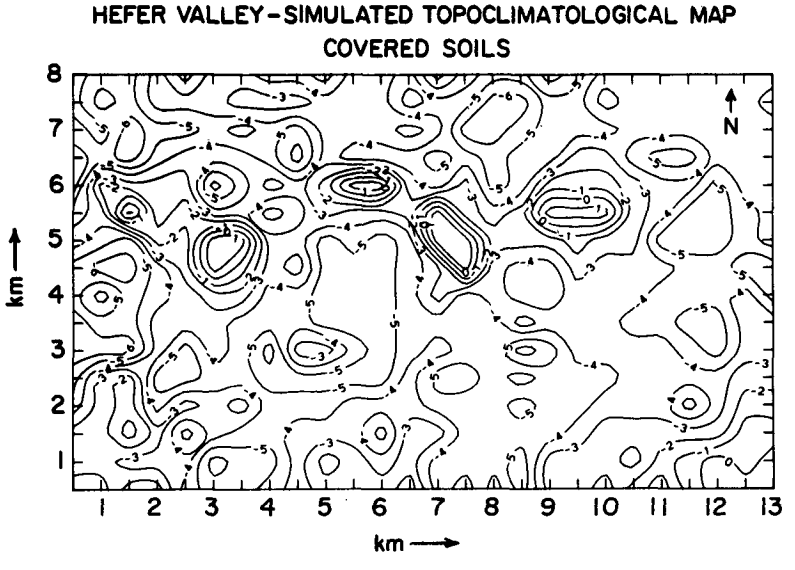

FIG. 16. Simulated topoclimatological map of minimum temperature in Hefer Valley.

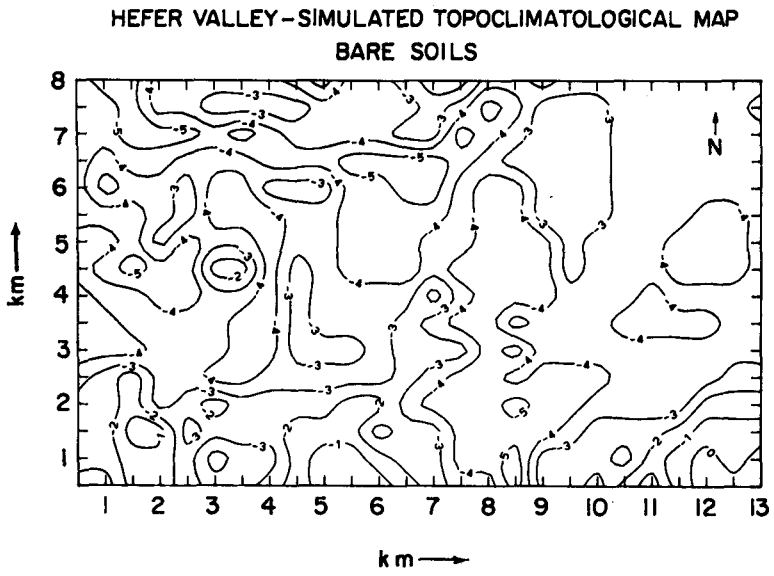

FIG. 17. As in Fig. 16 except for the bare Hefer Valley.

leading. Since this temperature varies during the different plant-developing stages, and with the different types of canopy, it seems that the only approach to provide appropriate data is by using models.

Other advantages which emphasize the potential use of a numerical model like the one presented in this study, are the possibility of studying the efficiency and energy requirements of various frost protection methods, and the possibility of obtaining immediate results (in comparison with topoclimatological surveys which have to be carried out for several years).

For an optimal exploitation of such a model, it may be helpful to set up a few observational stations in the studied domain which would be used for model validation. These observations should include measurements of radiation profiles of air temperature and humidity and profiles of wind velocity and direction in the lower atmosphere. Another attractive method available for testing the ability of the model to correctly predict the surface temperatures, is by carrying out temperature transects with airplane-mounted radiation thermometer as described, for example, by Nixon and Hales (1975). Also, high resolution images from satellite may be useful.

Finally, because of the large inhomogeneity in agricultural areas, a practical approach for obtaining boundary and initial conditions for the local-scale model is by using a larger-scale model.

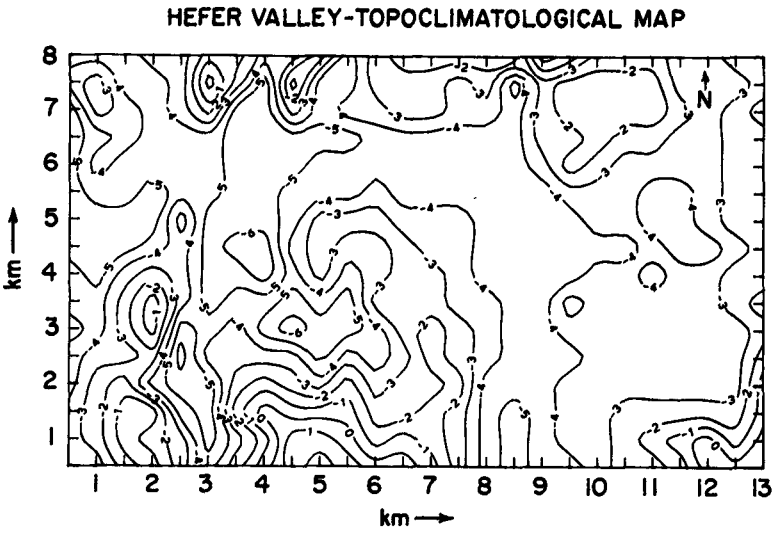

FIG. 18. As in Fig. 1, but with a resolution of 500 × 500 m.

Acknowledgments. This research was supported by the Israel Academy of Sciences and Humanities (Basic Research Foundation) and by the National Science Foundation under Grants ATM-8414181 and ATM-8616662. Computations were partly performed using the National Center for Atmospheric Research CRAY Computer (NCAR is sponsored by the NSF). The authors wish to thank the Meteorological Service of Israel for providing radiosondes and ground data related to their topoclimatological survey in Hefer Valley. They would also like to thank Roger A. Pielke, George Kallos and Ofir Naot for their review of the manuscript and for making valuable suggestions; Susan Einarsen and Linda Jensen for typing the manuscript; and Judy Sorbie for preparing the graphs.

REFERENCES

Avissar, R., and Y. Mahrer, 1988: Mapping frost-sensitive areas with a three-dimensional local scale model. Part I: Physical and numerical aspects. *J. Appl. Meteor.*, **27,** 400–413.

Bagdonass, A., J. C. Georg and J. F. Gerber, 1978: Techniques of frost prediction and methods of frost and cold protection. WMO Techn. Note No. 157, 160 p.

Blanc, M. L., H. Geslin, I. A. Holzberg and B. Mason, 1963: Protection against frost damage. WMO Techn. Note No. 51, 62 p.

Bootsma, A., 1976: Estimating grass minimum temperatures from screen minimum values and other climatological parameters. *Agric. Meteorol.*, **16,** 103–113.

Geiger, R., 1966: *The climate near the ground.* Harvard University Press, Cambridge, MA, 611 pp.

Goldsworthy, W. J., and M. D. Shulman, 1984: A statistical evaluation of near-ground frost processes. *Agric. For. Meteorol.*, **31,** 59–68.

Gross, G., 1987: Some effects of deforestation on drainage flow and local climate—A numerical study. *Bound. Lay. Meteorol.*, **38,** 315–337.

Hauf, T., and N. Witte, 1985: Fallstudie eines nachtlichen wind systems. *Met. Rdsch.*, **38,** 33–42.

Hogg, W. H., 1966: Air frost in spring at Long Ashton. Rep. Long Ashton Res. Stn., 1965, 290–298.

——, 1968: The duration of spring frosts on successive nights. Agric. Mem. No. 208.

Kalma, J. D., G. F. Byrne and M. E. Johnson, 1983: Frost mapping in southern Victoria: an assessment of HCMM thermal imagery. *J. Climatol.*, **3,** 1–19.

Lomas, J., and Z. Gat, 1971: Methods in agrotopoclimatic surveys—low temperatures. Agron. Rep. No. 1, Israel Meteorological Service, Bet-Dagan.

Nixon, P. R., and T. A. Hales, 1975: Observing cold-night temperatures of agricultural landscapes with an airplane-mounted radiation thermometer. *J. Appl. Meteorol.*, **14,** 498–505.

Ravikovitch, S., 1969: Soil map of Israel. Magnes. Hebrew University of Jerusalem. (In Hebrew).

Schnelle, F., 1950: Local climatic surveys according to frost damage to fruit culture. Deutscher Wetterdienst in der U.S. zone, *Berichte No. 12,* 99–104.

Suzuki, Y., S. Sato and K. Kawajiri, 1982: Frost damage and cold damage related to topographic climates in the warm region of Japan. Pt. 1, Distribution of maximum air temperatures on the slopes of Ube-Ono tea garden, Yamaguchi. *J. Agric. Meteorol. Tokyo,* **37,** 289–295.

Turrell, F. M., 1973: The science and technology of frost protection, Chap. 10. Citrus Industry III, Div. Agric. Sci., University of California, Berkeley, 383–446.

Von Lengerke, H. J., 1978: On the short-term predictability of frost and frost protection—A case study on Dunsandle Tea Estate in the Nilgiris (South India). *Agric. Meteorol.*, **19,** 1–10.

Zemel, Z., and J. Lomas, 1977: Soil temperature regime in Israel as a basis for agricultural planning and activity. Agromet. Rep. 8/77, Israel Meteorological Service, Bet-Dagan.